ESMO GOOD SCIENCE BETTER MEDICINE BEST PRACTICE

*Annals of Oncology* 29: 1853–1860, 2018
doi:10.1093/annonc/mdy218
Published online 6 June 2018

ORIGINAL ARTICLE

# Pathologic features of response to neoadjuvant anti-PD-1 in resected non-small-cell lung carcinoma: a proposal for quantitative immune-related pathologic response criteria (irPRC)

T. R. Cottrell[1], E. D. Thompson[1,2,3], P. M. Forde[2,3], J. E. Stein[4], A. S. Duffield[1], V. Anagnostou[2], N. Rekhtman[5], R. A. Anders[1,3], J. D. Cuda[1,4], P. B. Illei[1,2], E. Gabrielson[1,2], F. B. Askin[1], N. Niknafs[2], K. N. Smith[2,3], M. J. Velez[5], J. L. Sauter[5], J. M. Isbell[6], D. R. Jones[6], R. J. Battafarano[7], S. C. Yang[7], L. Danilova[3,8], J. D. Wolchok[9,10,11], S. L. Topalian[3,7], V. E. Velculescu[2,3], D. M. Pardoll[2,3], J. R. Brahmer[2,3], M. D. Hellmann[10,11,12], J. E. Chaft[10,12], A. Cimino-Mathews[1,2] & J. M. Taube[1,2,3,4,*]

[1]Department of Pathology, Johns Hopkins University SOM, Baltimore; [2]Department of Oncology, The Sidney Kimmel Comprehensive Cancer Center, Johns Hopkins University SOM, Baltimore; [3]The Johns Hopkins Bloomberg–Kimmel Institute for Cancer Immunotherapy, Baltimore; [4]Department of Dermatology, Johns Hopkins University SOM, Baltimore; [5]Department of Pathology; [6]Thoracic Surgery Service, Department of Surgery, Memorial Sloan Kettering Cancer Center, New York; [7]Department of Surgery, Johns Hopkins University SOM, Baltimore; [8]Division of Biostatistics and Bioinformatics, The Sidney Kimmel Comprehensive Cancer Center, Johns Hopkins University SOM, Baltimore; [9]Melanoma and Immunotherapeutics Service, Division of Solid Tumor Oncology, Department of Medicine, Ludwig Center for Cancer Immunotherapy, Memorial Sloan Kettering Cancer Center, New York; [10]Weill Cornell Medical College, New York; [11]Parker Institute for Cancer Immunotherapy, Memorial Sloan Kettering Cancer Center, New York; [12]Thoracic Oncology Service, Division of Solid Tumor Oncology, Department of Medicine, Memorial Sloan Kettering Cancer Center, New York, USA

*Correspondence to*: Dr Janis M. Taube, Division of Dermatopathology, Johns Hopkins University SOM, Blalock 907, 600 N. Wolfe St., Baltimore, MD 21287, USA. Tel: +1-410-955-3484; E-mail: jtaube1@jhmi.edu

**Background:** Neoadjuvant anti-PD-1 may improve outcomes for patients with resectable NSCLC and provides a critical window for examining pathologic features associated with response. Resections showing major pathologic response to neoadjuvant therapy, defined as ≤10% residual viable tumor (RVT), may predict improved long-term patient outcome. However, %RVT calculations were developed in the context of chemotherapy (%cRVT). An immune-related %RVT (%irRVT) has yet to be developed.

**Patients and methods:** The first trial of neoadjuvant anti-PD-1 (nivolumab, NCT02259621) was just reported. We analyzed hematoxylin and eosin-stained slides from the post-treatment resection specimens of the 20 patients with non-small-cell lung carcinoma who underwent definitive surgery. Pretreatment tumor biopsies and preresection radiographic 'tumor' measurements were also assessed.

**Results:** We found that the regression bed (the area of immune-mediated tumor clearance) accounts for the previously noted discrepancy between CT imaging and pathologic assessment of residual tumor. The regression bed is characterized by (i) immune activation—dense tumor infiltrating lymphocytes with macrophages and tertiary lymphoid structures; (ii) massive tumor cell death—cholesterol clefts; and (iii) tissue repair—neovascularization and proliferative fibrosis (each feature enriched in major pathologic responders versus nonresponders, $P < 0.05$). This distinct constellation of histologic findings was not identified in any pretreatment specimens. Histopathologic features of the regression bed were used to develop 'Immune-Related Pathologic Response Criteria' (irPRC), and these criteria were shown to be reproducible amongst pathologists. Specifically, %irRVT had improved interobserver consistency compared with %cRVT [median per-case %RVT variability 5% (0%–29%) versus 10% (0%–58%), $P = 0.007$] and a twofold decrease in median standard deviation across pathologists within a sample (4.6 versus 2.2, $P = 0.002$).

**Conclusions:** irPRC may be used to standardize pathologic assessment of immunotherapeutic efficacy. Long-term follow-up is needed to determine irPRC reliability as a surrogate for recurrence-free and overall survival.

**Key words:** neoadjuvant, PD-1, lung carcinoma, pathologic response, irPRC

## Introduction

Lung cancer is the leading cause of cancer death worldwide. Recent improvements in survival of patients with unresectable non-small-cell lung cancer (NSCLC) treated with PD-1/PD-L1 immune checkpoint blocking agents have generated interest in extending their use into the neoadjuvant setting. We recently published the results of a single arm, phase II clinical trial of neoadjuvant nivolumab in resectable stage I–IIIA NSCLC. In that study, while only 10% (2/20) of patients had radiographic objective responses by the time of surgical resection, 45% (9/20) of resected tumors showed a major pathologic response (MPR) [defined as ≤10% residual viable tumor (RVT) at the time of resection] using criteria for neoadjuvant chemotherapy (cMPR) [1]. (See Table 1 for terms and definitions related to pathologic response assessment.)

Due to the distinct mechanisms of action between conventional chemotherapy and immunotherapy, we hypothesized that the histopathologic features of pathologic response to immune checkpoint blockade may diverge from those reported for chemotherapy [2, 3], as suggested by anecdotal descriptions of tumor histology following anti-PD-1 [4, 5]. A standardized approach to the assessment of pathologic response is necessary for reliable interpretation of the post-treatment resection specimens in patients receiving neoadjuvant anti-PD-1 therapy and is particularly critical given the multitude of neoadjuvant immunotherapy clinical trials currently underway.

In the current study, we systematically assessed the features of histopathologic response to neoadjuvant anti-PD-1 in a previously described cohort of patients with NSCLC [6], and characterized features of immune-mediated tumor clearance. We then used the observed histologic features of immune-mediated regression to create a provisional scoring system for pathologic response to neoadjuvant anti-PD-1.

## Materials and methods

### Case selection

Post-treatment complete tumor resection and thoracic lymphadenectomy specimens were obtained from 20 patients with NSCLC who were treated on a phase II clinical trial (NCT02259621) of neoadjuvant nivolumab (anti-PD-1) at the Johns Hopkins Sidney Kimmel Comprehensive Cancer Center (SKCCC) and Memorial Sloan Kettering Cancer Center (MSKCC) [6]. Nine (45%) patients experienced a cMPR, including two (10%) patients with a pathologic complete response (pCR); seven (35%) had a partial pathologic response (>10% and <90% RVT by chemotherapy criteria; cRVT, supplementary Table S1, available at *Annals of Oncology* online) and four (20%) had a pathologic nonresponse (≥90% cRVT; pNR) (supplementary Figure S2, available at *Annals of Oncology*

**Table 1. Key terms, abbreviations, and definitions for assessing pathologic response to neoadjuvant therapy**

| Term | Description |
|---|---|
| Cholesterol clefts | Artifactual crystal-shaped spaces in tissue sections, indicative of insoluble (cell-membrane) lipid accumulation. Often associated with foreign-body giant cell reaction and 'foamy', i.e. lipid-laden macrophages. |
| Immune exclusion | Immune cells accumulate in the immediate peritumoral stroma, but do not infiltrate into the tumor parenchyma. A potential mechanism of resistance to immunotherapy. |
| Lymphoid aggregate | Discrete collection of >100 lymphocytes that does not demonstrate architectural organization or mixture of cell types of a TLS. |
| MPR (cMPR, irMPR) | ≤10% RVT remaining in post-therapy specimen. cMPR and irMPR are assigned using the chemotherapy and immunotherapy criteria, respectively. |
| Mature fibrosis | Established scar tissue. Fibroblasts are not as evident and are surrounded by large amounts of collagen. Low fibroblast to collagen ratio. |
| Neovascularization | Newly formed small blood vessels, most often seen in a background of tissue-repair. |
| Pathologic complete response (pCR) | No RVT remaining in post-therapy pathology specimen. |
| Pathologic NR (cNR, irNR) | ≥90% RVT remaining in post-therapy specimen. cNR and irNR are assigned when using the chemotherapy and immunotherapy criteria, respectively. |
| Proliferative (new) fibrosis | Characteristic of tissue repair/wound healing early stage when inflammatory cells release cytokines and growth factors that stimulate proliferation of fibroblast foci. High fibroblast to collagen ratio. |
| Regression bed | Area where tumor used to be, generated by immune-mediated tumor clearance. |
| RVT (cRVT, irRVT) | Percentage of viable tumor in post-therapy pathology specimen. cRVT and irRVT are the %RVT calculated by pathologists on the resection specimen using the chemotherapy and immunotherapy criteria, respectively. |
| TLS | Ectopic, organized lymphoid node-like structure that includes T cells, dendritic cells, activated B cells, high endothelial venules. |

online). The study schema and associated pathologic specimen analyses are shown in supplementary Figure S1, available at *Annals of Oncology* online. The institutional review boards at SKCCC and MSKCC approved this study, and all patients signed informed consent.

### Tumor bed identification by radiographic and gross pathologic correlation

The discrepancy between lesion size assessed on post-treatment CT scan and microscopic residual tumor amount has been previously reported for this cohort [6]. We hypothesized that this discrepancy could be due to the regression bed surrounding residual tumor. To test this hypothesis, the largest lesion diameter on post-treatment CT scan was compared with the largest diameter of the corresponding 'tumor mass' measured during routine surgical specimen gross examination for each patient.

### Histopathologic assessments of response to treatment

Details regarding specimen staging, pathologic assessment by chemotherapy response criteria, and the assessment of candidate immune and nonimmune histopathologic features related to immunotherapeutic response are provided in the supplementary Methods, available at *Annals of Oncology* online. Immune-related pathologic response criteria (irPRC) were developed using the features associated with response (detailed in Results section and supplementary Table S1, available at *Annals of Oncology* online). Four different pathologists not involved in the irPRC development and blinded to patient outcome first scored all specimens using the chemotherapy criteria (%cRVT), followed by a 2-week washout period. They were then trained on irPRC using one resection specimen. Each pathologist then independently scored the remaining 19 post-treatment resection specimens for residual viable tumor (%irRVT).

### Additional histopathologic assessments

Pretreatment tumors were evaluated for histopathologic features predictive of response to therapy. Primary tumor specimens were also studied for features that could possibly be associated with early relapse, and whether immune-mediated tumor clearance was more closely associated with a squamous cell or adenocarcinoma histology. Lymph nodes were studied for other histologic alterations beyond immune-mediated tumor clearance possibly related to anti-PD-1 administration. The presence of immune exclusion was assessed, supplementary Methods, available at *Annals of Oncology* online.

### Statistical analysis

Fisher's exact test was used to determine whether histopathologic features of immune-mediated regression were significantly enriched in pCR/cMPR specimens when compared with cNR specimens. Differences in the percentage of fibrosis were assessed using Student's *t* test. The comparisons of pathologic features between paired pre- and post-treatment specimens were evaluated using the McNemar test. Statistical analyses were carried out using R-software [7]. All tests were two-sided, and *P* values of $<0.05$ were considered as significant.

## Results

### Tumor bed identification by radiographic and gross pathologic correlation

A strong correlation was identified between the largest lesional diameter on the presurgical resection CT scan (taken post-immunotherapy), and the largest diameter measured during gross examination of the resection specimen by pathology (Figure 1A and B). Microscopic examination of the 'tumor mass' revealed that the composition ranged from complete replacement of tumor by fibroinflammatory areas of immune-mediated regression (referred to here as 'regression beds') in patients with pCR, to masses composed nearly entirely of viable tumor, consistent with no treatment response (Figure 1C).

### Histopathologic features of immune-mediated regression in NSCLC resection specimens

The regression bed is characterized by dense immune infiltrates with features of activation [tertiary lymphoid structure (TLS), dense tumor infiltrating lymphocytes (TIL) infiltrates and plasma cells, granuloma formation], along with features of cell death (cholesterol clefts, interstitial foamy macrophages), and tissue repair/wound healing, such as neovascularization and new, proliferative fibrosis (Figure 2A). These features were absent or rarely present in specimens from nonresponders. In particular, the percent of the tumor bed surface area occupied by new fibrosis and the presence of neovascularization were two of the key distinguishing features between cMPR specimens versus specimens showing cNR to therapy ($P \leq 0.001$ for both; Figure 2B). In contrast to TLS, unstructured lymphoid aggregates were present in specimens from both responders and nonresponders (NR). The features of cell death such as necrosis, cholesterol clefts, giant cells, and foamy macrophages, as well as acellular fibrosis and mixed inflammatory infiltrates, have been previously reported in specimens from patients treated with neoadjuvant chemotherapy [2, 8]. However, the specific immunologic features of TLS and dense plasma cells accompanied by the proliferative fibrosis and neovascularization of wound healing/tissue repair have not been detailed in chemotherapy patients and may reflect the different mechanism of action of immunotherapeutic agents.

Following the nomination of immune-mediated features of regression identified when comparing the two extremes of the cohort (pCR/cMPR versus cNR specimens), all specimens were then individually assessed for each feature. Most cases showing any degree of response exhibited a moderate to severe grade of TIL in association with a number of the other histologic findings, most commonly neovascularization, proliferative fibrosis, dense plasma cells, cholesterol clefts, and TLS (Figure 3A). An 'outside-in' pattern of regression was typically present, meaning that regression beds were observed surrounding residual tumor and abutting normal background lung tissue (Figure 3B and C). The peripheral location of the regression bed has important implications for how specimens are sampled for histologic analysis and how the total tumor bed area is defined microscopically.

The distinct features of immune-mediated regression observed in the lung were also observed in the resected draining lymph nodes from two patients (patients 4 and 13) (Figure 3D). Based on pretreatment imaging, only one of those patients (patient 13) was suspected to have nodal involvement, with neither having pathologically confirmed pretreatment nodal disease.

### irPRC: a novel scoring system

Following identification of pathologic features of response to anti-PD-1 therapy, irPRC were developed (supplementary Table S1, available at *Annals of Oncology* online). Using this approach,

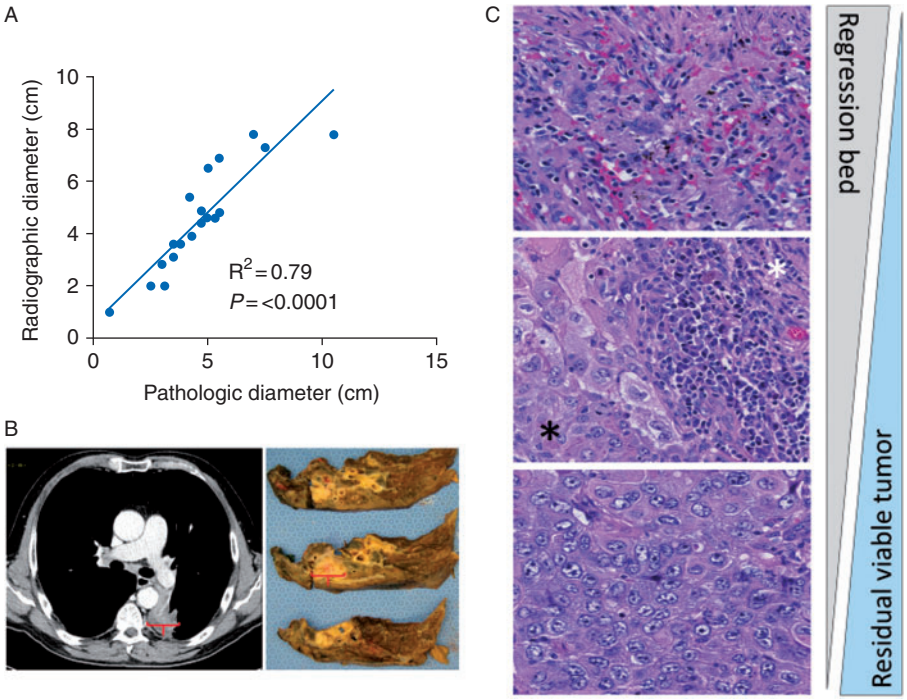


**Figure 1.** Radiographic and gross pathologic measurements of 'tumor mass' include areas of immune-mediated tumor regression. (A) There is a significant correlation between the radiographic measurement of the post-treatment lung mass on CT scan and pathologic measurement of the mass in the resected lung specimen. The grossly measured mass includes the microscopically evident regression bed. (B) Representative example of post-neoadjuvant anti-PD-1 treatment lung mass measured on CT scan and the corresponding resected lung specimen. The mass measures ~3.8 cm in greatest dimension by both modalities, though microscopic examination shows the mass is composed of only 50% RVT. (C) Microscopic examination reveals post-treatment lung masses are composed of varying proportions of fibroinflammatory regression stroma and RVT. Representative photomicrographs from a complete pathologic responder (top), partial pathologic responder (middle; residual tumor with black asterisk, regression bed with white asterisk), and tumors showing no treatment effect (bottom). Original magnification: ×400, all panels.

%irRVT = viable tumor area/total tumor bed area, whereby the total tumor bed = regression bed + RVT + necrosis (Figure 4A). If multiple primary tumor foci are present, the areas from each are summed such that the %irRVT is a representation of the total primary tumor burden. Due to the distinct histologic features of immune-mediated regression, it may also be possible to score %irRVT in lymph nodes (supplementary Figure S3, available at *Annals of Oncology* online).

## Interpathologist reproducibility of scoring %cRVT and %irRVT

Interpathologist variability when scoring specimens for RVT in NSCLC patients treated with neoadjuvant anti-PD-1 was assessed. Four pathologists scored 19 post-treatment specimens for %cRVT and %irRVT (Figure 4B). Compared with %cRVT, %irRVT had a twofold decrease in median standard deviation of scores across pathologists within a sample (4.6 versus 2.2, $P = 0.002$) and improved interobserver consistency [median per-case %RVT variability 5% (0%–29%) versus 10% (0%–58%), $P = 0.007$; Figure 4C].

## Additional histopathologic findings

Refer to the supplementary Results, available at *Annals of Oncology* online for details related to immune exclusion, early disease recurrence, response assessment by tumor histologic subtype and pretreatment tumor features, as well as histologic features of tumor-devoid lymph nodes. Briefly, 1 of the 20 assessed post-treatment tumors showed evidence of lymphocyte exclusion following anti-PD-1 therapy (supplementary Figure S4, available at *Annals of Oncology* online). Reactive histologic features in non-tumor bearing lymph nodes did not differ between responding and nonresponding patients (supplementary Figure S5, available at *Annals of Oncology* online).

# Discussion

Immune checkpoint blockade in the neoadjuvant setting represents one of the next frontiers in cancer immunotherapy. Clinical trials are underway for patients with NSCLC and multiple other solid tumor types; however, it will be years before survival outcomes are available. MPR has been put forth as a surrogate for survival in lung cancer patients receiving neoadjuvant chemotherapy [9], and scoring systems for calculating the %cRVT in that setting have been recommended [8, 9]. Assessment of pathologic response has the advantage of providing an early indication of therapeutic efficacy within weeks or months instead of waiting years to accrue survival data [10, 11]. It may also allow physicians to determine whether or not additional adjuvant therapy is necessary postresection.

A

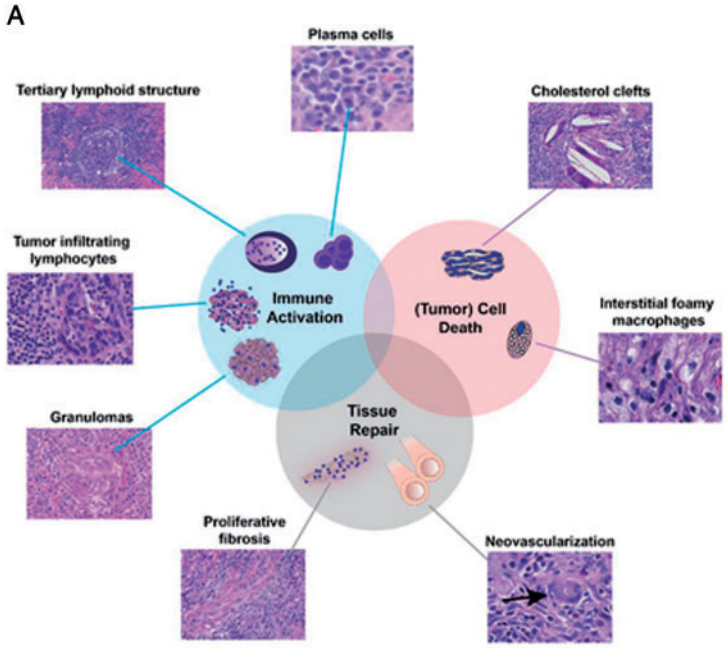


B

| Feature, *n* (%)[a] | cMPR (*n* = 9) | cNR (*n* = 4) | *P* value[b] |
|---|---|---|---|
| Fibrosis | | | |
| % Fibrosis, Median (range) | 75 (40-96.5) | 0 (0-0) | 2.2e-05[c] |
| Proliferative Fibrosis | 7 (78) | 0 (0) | 0.021 |
| Mature Fibrosis | 1 (11) | 0 (0) | 1 |
| Mixed Fibrosis | 1 (11) | 0 (0) | 1 |
| Neovascularization | 9 (100) | 0 (0) | 0.0014 |
| Cholesterol clefts | 8 (89) | 0 (0) | 0.007 |
| TIL score | | | |
| Low (1+) | 0 (0) | 3 (75) | 0.014 |
| High (3+) | 7 (78) | 0 (0) | 0.021 |
| Tertiary lymphoid structures | 7 (78) | 0 (0) | 0.021 |
| Dense plasma cells | 6 (67) | 0 (0) | 0.07 |
| Granulomas | 5 (56) | 0 (0) | 0.1 |
| Foamy macrophages | | | |
| Interstitial | 4 (44) | 0 (0) | 0.23 |
| Alveolar | 8 (89) | 2 (50) | 0.2 |
| Giant cells | 7 (78) | 1 (25) | 0.22 |
| Lymphoid aggregates | 9 (100) | 3 (75) | 0.31 |
| Necrosis | 3 (33) | 0 (0) | 0.5 |
| Hemosiderin | 5 (56) | 2 (50) | 1 |
| Neutrophils | 3 (33) | 1 (25) | 1 |

[a]All features are reported as *n* (%) of patients with the feature present, unless otherwise noted.
[b]Fisher's Exact test, unless otherwise noted.
[c]Student's t-test

**Figure 2.** Histologic features of pathologic response to neoadjuvant anti-PD-1 in NSCLC. (A) Post-treatment NSCLC specimens with MPR to therapy showed a distinct pattern of immune-mediated tumor regression, characterized by histologic features of immune activation, tumor cell death, and tissue repair. (B) Association of individual histologic features with MPR/complete pathologic response.

Immunotherapies have a mechanism of action distinct from chemotherapy. Here, we systematically identify the histopathologic features of treatment response to anti-PD-1 and use them to form the basis of a novel scoring system. Recognition of the specific histologic features of immune-mediated regression, a.k.a 'the regression bed', promoted higher reproducibility amongst the pathologists, which will be key in accurately predicting outcomes for individual patients and facilitating comparisons between different clinical trials [12]. It is possible that a %irRVT different than the 10% threshold associated with cMPR will be associated with improved progression-free and/or overall survival in this setting, especially if immunotherapy has the anticipated effect of driving improved outcomes by suppressing or eradicating micrometastatic disease.

We also explicitly demonstrated that the regression bed accounts for the previously reported discrepancy between radiographic response and pathologic response [6]. Specifically, 18 out of the 20 patients assessable for pathologic response had stable disease and the remaining 2 patients had a partial response by RECIST 1.1 assessment, despite varying amounts of RVT identified microscopically. These findings support using a 'disease control' metric, which includes patients with 'stable disease' along with objective responders (complete and partial radiographic responders by RECIST) when assigning patients to categories of response versus nonresponse. It remains to be determined whether nuanced signals on PET-CT or other sophisticated imaging approaches can be used to distinguish between regression bed and residual tumor.

To date, most studies that have analyzed post-treatment tumor specimens from patients with advanced cancer treated with anti-PD-1 have focused on the effector role of cytotoxic T-lymphocytes in tumor eradication. Notably, the neoadjuvant setting provides a unique window for studying drug mechanism of action. In the post-treatment resection specimens from responders, not only were dense TILs observed, but plasma cells and TLS were also enriched. TLS are thought to be key for supporting both local and systemic T- and B-cell antitumor responses [13]. Additionally, B cells are thought to be involved in accelerating

A

| | cMPR | | | | | | | | | cPR | | | | | | | cNR | | | |
|---|---|---|---|---|---|---|---|---|---|---|---|---|---|---|---|---|---|---|---|---|
| Patient # | 1 | 2 | 3 | 4 | 5 | 6 | 7 | 8 | 9 | 10 | 11 | 12 | 13 | 14 | 15 | 16 | 17 | 18 | 19 | 20 |
| TIL Score | 3+ | 3+ | 3+ | 3+ | 2+ | 3+ | 3+ | 2+ | 3+ | 2+ | 1+ | 3+ | 3+ | 1+ | 3+ | 2+ | 2+ | 1+ | 1+ | 1+ |
| Neovascularization | + | + | + | + | + | + | + | + | + | + | - | + | + | - | - | - | - | - | - | - |
| Proliferative fibrosis | + | + | + | + | + | - | + | + | + | + | - | + | + | + | + | - | - | - | - | - |
| Cholesterol clefts | + | + | + | + | + | + | + | + | - | + | - | + | + | - | - | - | - | - | - | - |
| Tertiary lymphoid structures | + | + | - | + | + | + | + | - | + | - | + | + | + | - | + | - | - | - | - | - |
| Dense plasma cells | - | - | - | + | + | + | + | + | + | + | + | + | + | - | + | + | - | - | - | - |
| Granulomas | + | + | - | + | - | + | - | + | - | + | - | - | - | - | - | - | - | - | - | - |
| Giant Cells | + | + | - | + | + | + | - | + | + | + | + | + | + | - | - | - | - | - | - | + |
| Interstitial foamy macrophages | - | - | + | + | + | - | + | - | - | - | - | + | - | - | - | - | - | - | - | - |
| Histologic type | Adeno | Adeno | Other | SCC | Adeno | Adeno | Adeno | Adeno | SCC | SCC | SCC | SCC | Other | SCC | Adeno | Adeno | Adeno | Adeno | Adeno | Adeno |

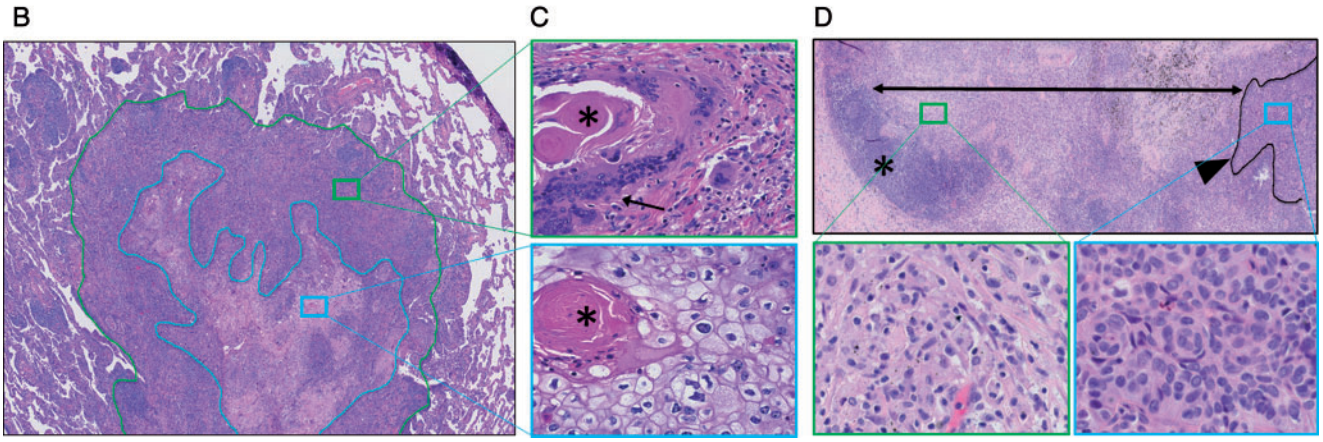


**Figure 3.** Individual features of pathologic response co-localize in the regression bed surrounding residual tumor. (A) Features of pathologic response identified in MPR specimens are also present in the regression bed of 'partially responding tumors'. However, the tumors from patients 11, 14, and 16 (black box outlines on heat map) had minimal features suggestive of immune-mediated regression. These cases were notable for immune exclusion (patient 11, see Figure 5) and disease relapse (patients 14 and 16). (B) Photomicrograph of a partial responder with 30% cRVT (blue outline). The regression bed (green outline) typically surrounds the residual tumor foci, suggesting an 'outside-in' pattern of tumor regression. (C) A patient with a partially responding keratinizing, squamous cell NSCLC (bottom panel) had a regression bed containing residual keratin pearls (top panel, asterisk), further supporting the interpretation of this distinctive peritumoral region as 'regression bed'. (D) Features of immune-mediated pathologic response may also be identified in lymph nodes, as shown here for patient 4. The double-headed arrow denotes the extent of the regression bed, which is positioned between normal lymph node tissue (asterisk) and RVT (black outline). These findings are notable, as they suggest that immune-mediated responses can be identified and potentially quantified using irPRC, even in tissues normally rich in immune cells. Additionally, the histologic features of regression bed are distinctive enough that responses in previously undiagnosed microscopic disease may also potentially be estimated. Original magnifications: (B) ×20, (C) ×400, (D) ×20 (top panel), and ×200 (bottom panels).

wound healing, and have been associated with neoangiogenesis and new fibrosis [14], both of which are key features observed in the regression beds formed during immune-mediated tumor regression. Other immune cell subsets, including T-regs, Th2, and M2 cells, as well as cells dying from the so-called 'immunogenic cell death' have also been implicated in stimulating tissue repair [15–17], highlighting the complex interplay between specific immune cell subsets, tumorigenesis, tumor cell death, and tissue repair and regeneration.

The extent of immune-mediated tumor clearance in this cohort may largely be a function of the interval between treatment initiation and definitive resection. Histologic patterns suggestive of antigenic but incompletely eliminated tumors were observed. Either with more time, or with additional immunotherapy, there may have been more extensive or complete tumor clearance in these thoroughly immune-infiltrated tumors. Interestingly, we identified a post-treatment tumor with a striking pattern of immune exclusion. Activation of the canonical β-catenin pathway has been associated with T-cell exclusion in melanoma, bladder cancer, and ovarian carcinoma [18–20] and may therefore be implicated in the pattern of immune exclusion identified in our study. In the neoadjuvant setting, when the resistant clone is confined to the primary tumor bed, clearance is likely achieved by the definitive resection surgery. However, if micrometastases of the resistant clone have seeded, these patients may require strategic adjuvant approaches, e.g. chemotherapy, stimulator of interferon genes complex (STING) agonists, or even β-catenin inhibitors [21, 22].

Standardized assessments of %RVT have the potential to facilitate trial design and accelerate drug development. However, it is

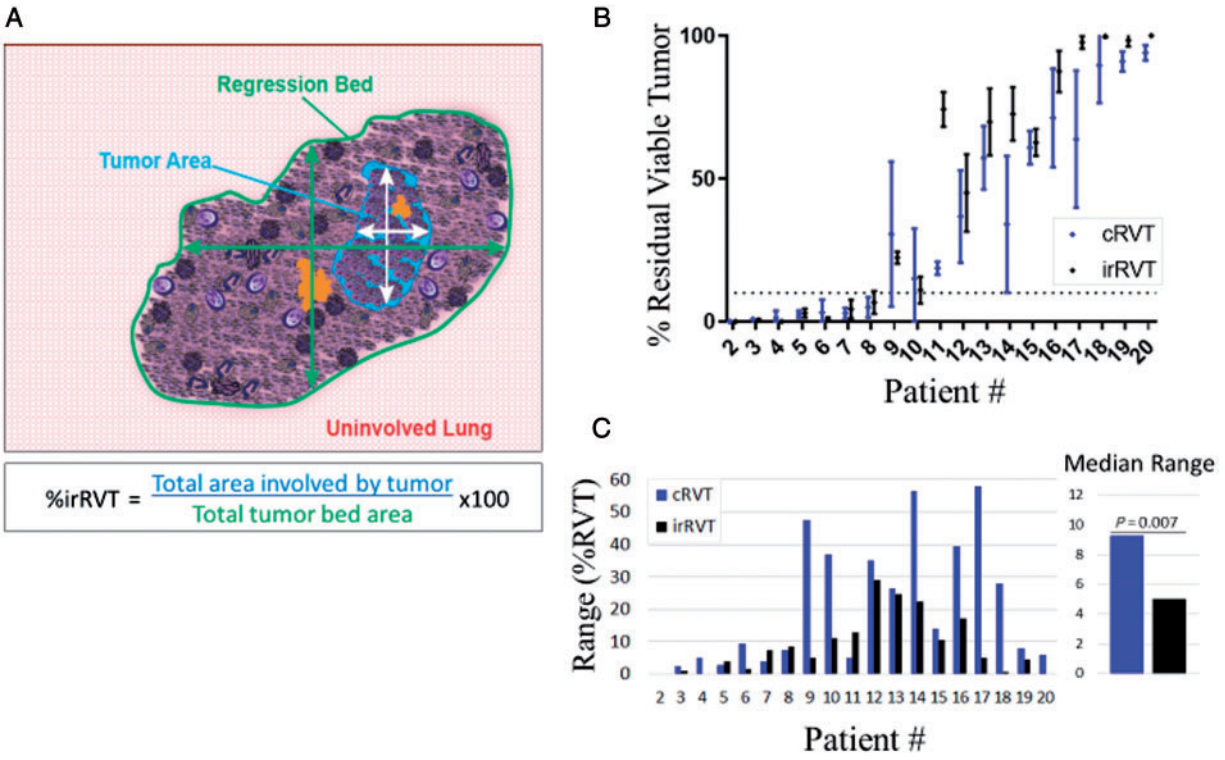


**Figure 4.** Proposal for reproducible, quantitative irPRC. (A) %irRVT is assessed by dividing the total surface area of RVT (circled in blue) by the total tumor bed area ×100. The total tumor bed area (circled in green) is composed of the regression bed area+RVT area+areas of necrosis (supplementary Table S1, available at *Annals of Oncology* online). The lymph node RVT (LN-irRVT) is calculated separately, but using the same approach, i.e. by measuring the cross-sectional area of RVT and dividing by total tumor bed area. If there are multiple lymph node foci, the areas of each component are summed together to give a %LN-irRVT that represents the total tumor burden in all the lymph nodes assessed. (B) irPRC improves interpathologist reproducibility for percent RVT (%irRVT). Four pathologists blinded to clinical outcome were trained on the tumor from patient 1, and then scored tumors from patients 2 to 20 by both irPRC and chemotherapy criteria. The mean±SD %irRVT and %cRVT scores for each case are shown in black and blue, respectively. Strong concordance was observed among pathologists for the specimens with very little residual tumor when using either the chemotherapy criteria or irPRC. In contrast, large discrepancies in scores for %cRVT were seen in specimens from partial responders. (C) The interpathologist variability in scoring of each case is presented as the range of %RVT scores from four pathologists using the chemotherapy (cRVT) and immune-related (irRVT) criteria (left), shown by blue and black lines, respectively. For each method, the median overall range is presented (right). The proposed immune-related response criteria significantly reduce interpathologist variability in scoring relative to the chemotherapy criteria in these post-immunotherapy specimens.

important to note that %cRVT as a surrogate of survival was validated in the setting of neoadjuvant chemotherapy. While we have outlined a proposed approach to assessment of %irRVT in patients receiving immunotherapy, these findings will need to be confirmed when parameters such as long-term disease-free and overall survival become available on this cohort, and through future clinical trials with larger patient cohorts in the phase II and III settings. Based on our findings in this study, we suggest sampling a full cross-section of tumor through the largest dimension to facilitate the most-accurate assessment of immune-mediated tumor regression, supplementary Figure S6, available at *Annals of Oncology* online. We also suggest the minimum pathologic parameters gathered should include those in the Case Report Form (supplementary Table S3, available at *Annals of Oncology* online), enabling longer-term assessments to be made regarding which pathologic features are most closely linked to long-term outcomes. Similar assessments will be required when neoadjuvant immunotherapy is administered to patients with other tumor types, and when immunotherapy is combined with chemotherapy and other antitumor agents.

## Acknowledgements

The authors would like to thank Dr Cyrus Hedvat for helpful discussions and Dr Robin Edwards for thoughtful review of the manuscript (both BMS), Dr Alex Baras and Peter Nguyen (both JHU) for slide scanning and website creation, Aleksandra Ogurtsova and Haying Xu for multiplex staining, RT Tracy (JHU) for assistance with technical drawings, and Cliff Hoyt and Kent Johnson (Perkin-Elmer) for assistance with the Vectra image displays.

## Funding

This work was supported by Bristol-Myers Squibb and the International Immuno-Oncology Network (JMT, SLT, DMP, and clinical trial investigators); Sidney Kimmel Cancer Center Core Grant P30 CA006973 (JMT); National Cancer Institute R01 CA142779 (JMT, SLT, DMP); NIH T32 CA193145 (TRC); LCFA/IASLC grant #125133 (KNS); CA121113 (VEV, VA);

CA180950 (VEV); the LUNGevity Foundation (VA, PMF); the V Foundation (VA); the MacMillan Foundation (VA); the International Association for the Study of Lung Cancer, Prevent Cancer & ECOG-ACRIN (PMF); Memorial Sloan Kettering Cancer Center Core Grant NIH P30 CA008748 (all MSKCC investigators). The Johns Hopkins Bloomberg-Kimmel Institute for Cancer Immunotherapy; and Stand Up To Cancer–Cancer Research Institute Cancer Immunology Translational Cancer Research Grant SU2C-AACR-DT1012. Stand Up To Cancer is a program of the Entertainment Industry Foundation administered by the American Association for Cancer Research.

## Disclosure

EDT, PMF, JDC, EG, JDW, JRB, AC-M: Bristol-Myers Squibb. RAA: Bristol-Myers Squibb, Merck, Five Prime Therapeutics, and Adaptive Biotechnologies. PBI: Genentech; Roche, AstraZeneca, Bristol-Myers Squibb, and AbbVie. JLS: Merck. SLT: Research grants from Bristol-Myers Squibb; consulting and stock, Five Prime Therapeutics. VEV: Personal Genome Diagnostics; Ignyta. DMP: Research grants from Bristol-Myers Squibb; patent royalties through institution, Bristol-Myers Squibb and Potenza Therapeutics; and consulting, Amgen, Merck, MedImmune, Five Prime Therapeutics, and Potenza Therapeutics. MDH: Bristol-Myers Squibb, Merck, AstraZeneca, Genentech/Roche, Janssen, Novartis, Mirati, and Shattuck Labs. JEC: Bristol-Myers Squibb, Merck, AstraZeneca, and Genentech. JMT: Bristol-Myers Squibb, Amgen, AstraZeneca, and Merck. TRC, JES, ASD, VA, NR, FA, NN, KNS, MV, JMI, DRJ, RB, SCY, and LD have declared no conflicts of interest.

## References

1. Forde PM, Chaft JE, Smith KN et al. Neoadjuvant PD-1 blockade in resectable lung cancer. N Engl J Med 2018; 378: 1976–1986.
2. Yamane Y, Ishii G, Goto K et al. A novel histopathological evaluation method predicting the outcome of non-small cell lung cancer treated by neoadjuvant therapy: the prognostic importance of the area of residual tumor. J Thorac Oncol 2010; 5(1): 49–55.
3. Liu-Jarin X, Stoopler MB, Raftopoulos H et al. Histologic assessment of non-small cell lung carcinoma after neoadjuvant therapy. Mod Pathol 2003; 16(11): 1102.
4. Topalian SL, Sznol M, McDermott DF et al. Survival, durable tumor remission, and long-term safety in patients with advanced melanoma receiving nivolumab. J Clin Oncol 2014; 32(10): 1020–1030.
5. Le DT, Uram JN, Wang H et al. PD-1 blockade in tumors with mismatch-repair deficiency. N Engl J Med 2015; 372(26): 2509–2520.
6. Forde PM, Chaft JE, Smith KN et al. Neoadjuvant PD-1 blockade in resectable lung cancer. N Engl J Med 2018; 378: 1976–1986.
7. R Core Team. A Language and Environment for Statistical Computing. Vienna, Austria: R Core Team 2004.
8. Pataer A, Kalhor N, Correa AM et al. Histopathologic response criteria predict survival of patients with resected lung cancer after neoadjuvant chemotherapy. J Thorac Oncol 2012; 7(5): 825–832.
9. Hellmann MD, Chaft JE, William WN Jr et al. Pathological response after neoadjuvant chemotherapy in resectable non-small-cell lung cancers: proposal for the use of major pathological response as a surrogate endpoint. Lancet Oncol 2014; 15(1): e42–e50.
10. Prowell TM, Pazdur R. Pathological complete response and accelerated drug approval in early breast cancer. N Engl J Med 2012; 366(26): 2438–2441.
11. Peres J. Neoadjuvant trials could speed up drug approvals. J Natl Cancer Inst 2014; 106(3): dju072.
12. Provenzano E, Bossuyt V, Viale G et al. Standardization of pathologic evaluation and reporting of postneoadjuvant specimens in clinical trials of breast cancer: recommendations from an international working group. Mod Pathol 2015; 28(9): 1185–1201.
13. Dieu-Nosjean MC, Giraldo NA, Kaplon H et al. Tertiary lymphoid structures, drivers of the anti-tumor responses in human cancers. Immunol Rev 2016; 271(1): 260–275.
14. Sirbulescu RF, Boehm CK, Soon E et al. Mature B cells accelerate wound healing after acute and chronic diabetic skin lesions. Wound Repair Regen 2017; 25(5): 774–791.
15. Kumar S, Calianese D, Birge RB. Efferocytosis of dying cells differentially modulate immunological outcomes in tumor microenvironment. Immunol Rev 2017; 280(1): 149–164.
16. Fuchs Y, Steller H. Live to die another way: modes of programmed cell death and the signals emanating from dying cells. Nat Rev Mol Cell Biol 2015; 16(6): 329–344.
17. Green JA, Arpaia N, Schizas M et al. A nonimmune function of T cells in promoting lung tumor progression. J Exp Med 2017; 214(12): 3565–3575.
18. Spranger S, Bao R, Gajewski TF. Melanoma-intrinsic beta-catenin signalling prevents anti-tumour immunity. Nature 2015; 523(7559): 231–235.
19. Sweis RF, Spranger S, Bao R et al. Molecular drivers of the non-T-cell-inflamed tumor microenvironment in urothelial bladder cancer. Cancer Immunol Res 2016; 4(7): 563–568.
20. Jimenez-Sanchez A, Memon D, Pourpe S et al. Heterogeneous tumor-immune microenvironments among differentially growing metastases in an ovarian cancer patient. Cell 2017; 170(5): 927–938 e920.
21. Woo SR, Fuertes MB, Corrales L et al. STING-dependent cytosolic DNA sensing mediates innate immune recognition of immunogenic tumors. Immunity 2014; 41(5): 830–842.
22. Spranger S, Luke JJ, Bao R et al. Density of immunogenic antigens does not explain the presence or absence of the T-cell-inflamed tumor microenvironment in melanoma. Proc Natl Acad Sci USA 2016; 113(48): E7759–E7768.